
**International Journal of Control Theory and Applications**

ISSN : 0974-5572



**Volume 10 • Number 36 • 2017**

# Cascaded qZS Multilevel Inverter with DTFC Scheme for Soft Starting Induction Motor

**R. Murugesan[a] and M. Manikandan[b]**

[a]*Research scholar, Department of Electrical and electronics engineering, St.Peter's University, Chennai, Tamilnadu, India. Email: rmurugesanphd@gmail.com*
[b]*Associate Professor, Department of Electronics and Communication engineering, Anna University, Chennai, Tamilnadu, India. Email: maniiz@yahoo.com*

***Abstract:*** This paper proposed a three-phase quasi Z-source cascade multilevel-inverter for induction motor application. A qZS-CMI's fed induction motor drive operating under direct torque and flux control (DTFC). The proposed control scheme has achieves soft start capability in induction motor, generally, Quasi Z-source allows continuous input current, improved reliability of the system. But the main aim of the paper, the generated residential DC voltage gain increased without using any dc/dc converter, which is also reduce the passive component stress significantly to perform at same voltage boost up condition, and has inherent limitation of inrush current at startup stage. The shoot-through ratio is very small ($1 > D > 0$). Additionally, the cascaded H-bridge inverter is employed to reduces voltage balancing problem at load feed conditions. Therefore, the inverter can improves system efficiency and improving motor performance by DTFC controller. This technique improves soft starting of the drive. Simulation results have revealed that, the proposed DTFC soft startup strategy is suppressed the inrush surge current. Experiment is carried out on a 7-level voltage output, qZS-CMI based MIC-fed IM drives exhibit interesting performance.

***Keywords:*** Three-phase Quasi-Z-source inverter; cascade multilevel inverter; direct torque and flux control (DTFC); induction motor drives.

## 1. INTRODUCTION

Asynchronous motor or induction motor drives are generally used in industrial application for heavy load applications. Since, they are more rugged, reliable, compact, and more efficient and also cheaper which is compared with other dc machines. However, difficulties in improving performance of induction motor, as the machine model is complicated, highly coupled, nonlinear, multivariable and uncertain (J. M. Carrasco, L. G. Franquelo, *et. al.,* Aug. 2006). Prolonged passage of large current through the motor during start stage can be cause the steep temperature raises resulting in failure of the insulation of the motor winding. So need to limit a stator current initially on induction motor drive. Soft stat of induction motor drives are generally used in fault timing and high torque ripple problem to compensate fault and ripples of high torque ripples control. Additional

merits of soft start process on induction motors is offers a less mechanical stress of components and improving equipment life. Speed and torque performance is been improved by toque and flux control scheme so here combined form of direct torque and flux control is used in this paper in order to reducing complexity of control. This control is usually provided through Field Oriented Control (FOC) (Singh, G.K. April 1994), its covers a torque control based reference generation and flux control based reference current generation for pulse width modulation using parks transformation. Current-regulated pulse-width-modulation inverter and inner current loops reduce the dynamic occurrence in the operating methods wherein the voltage margin is insufficient for the current control, specifically in the field weakening section (L.Tang, L.Zhong, *et. al*., 2002).

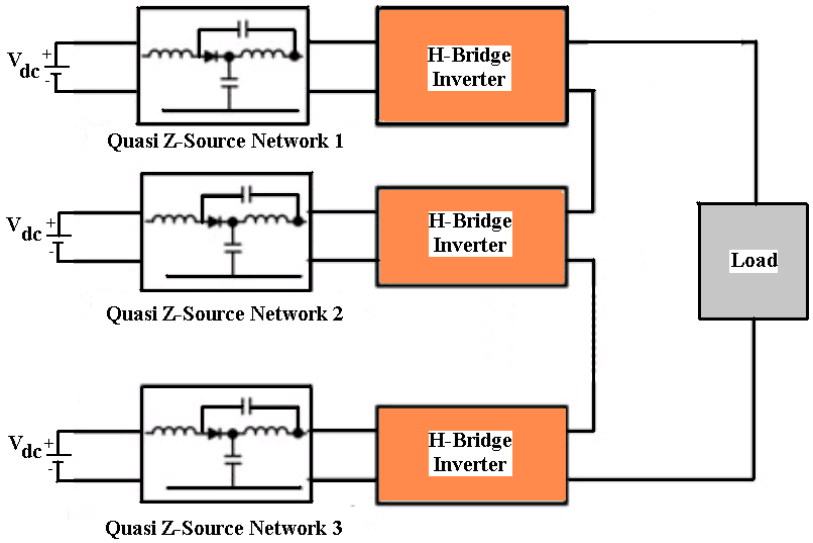


**Figure 1: Proposed MICs based on cascaded QZS fed induction motor**

The proposed Direct Torque and Flux Control (DTFC) are used to reduce a complexity of classical torque flux control and also provide an improved torque and flux control performance without need of additional control structures. DTFC provides a control of flux, torque and speed amplitude control (I.Takahashi, *et. al.,* March/ April, 1989 - A. Merabet, *et. al.,* 2006).

The proposed quasi-impedance source cascaded multilevel inverter (qZS-CMI) based on MICs fed load arrangement is shown in the Figure 1. Multilevel inverter schemes are applied on proposed Induction drives control (M. Calais and V. Agelidis, Jul. 1998– M. Shen, A. Joseph, Y. Huang, *et. al*., Aug. 14–16, 2006). Where intelligent QZS method is used to avoid the harmonic current and also decreases the inrush current in starting time of the motor, which is mainly avoid the starting time heavy torque; since generally the asynchronous motors have self starting and their starting current is greater than the running time current (D.Seyoum, *et. al., .,* Jun. 2003). Whereas the torque is directly proportional to the current and the torque also increased (G. Zenginobuz, *et. al.,* June 2004).

The cascaded H-bridge structure can reduce the voltage gain requirement for each module, as well as harmonic level. Additionally the single-stage energy conversion and higher equivalent output pulse width modulation (PWM) frequency strategy has enhanced the drive performance. A generalized inverter scheme gives a regulated AC voltage from constant direct current. Here boosting factors is achieved using load transformer and front end boost converter. The module number can be optimized regarding the inverter efficiency. Moreover, the drive reliability is highly enhanced compared with the cascaded H-bridge inverter, because the ZSI is immune to the shoot-through faults. The minimization of stress is achieved through passive components size and count reduction (L. Liu, *et. al.,* Sep. 2011- Y. Liu, *et. al.,* Feb. 2014).

In order to improving the performance of proposed inverter schemes is achieved by Direct Torque and Flux Control (DTFC) in this paper. This technique is proposed to achieve soft starting condition in drive. And also gives a better speed control performance. Compared with conventional method; which has produce better controlling action to the motor; the effect of the stator resistance is estimated using a PI estimator. Operation of DTFC is extended to high speed region using field weakening strategy. Flux linkage and torque is derived by proportional integral (PI) which is used for DTFC control loop. Instability of system is obtained by difference between stator resistance on controller and motor.

## 2. QZSI MODULE DESIGN

In order to design the quasi-Z-source network and analyze the power loss, the voltage and current of the capacitors, inductors, and switching devices need to be derived. The optimization method is uses to calculate for finding parameters for active and passive elements in present inverter configuration. The qZSI has three different operation states, called as active state, zero state, and shoot-through state. The equivalent circuits of the qZSI module during different modes. This is shown in Figure 2,

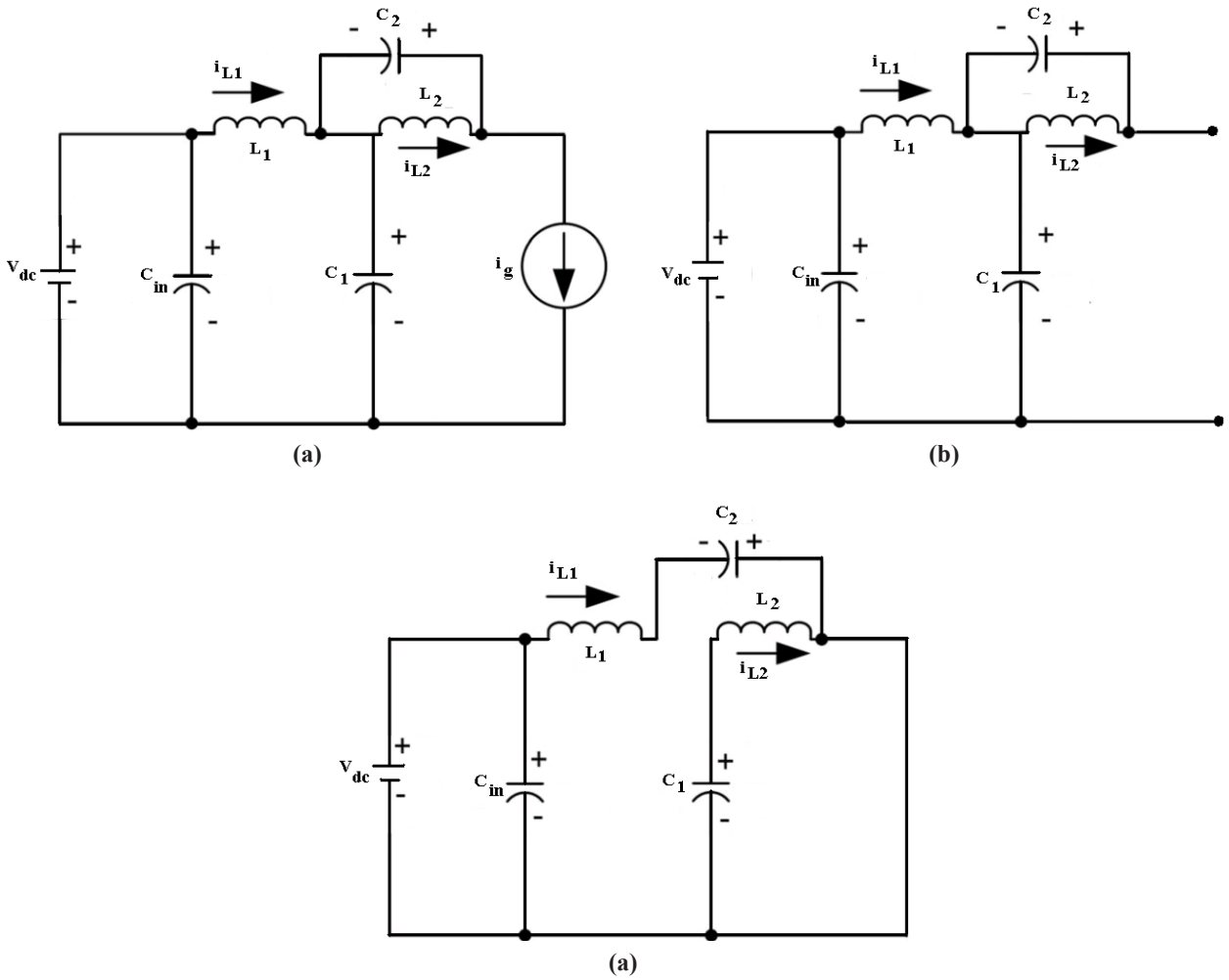


**Figure 2: Different operation modes of the qZSI (a) active state, (b) zero state, and (c) shoot-through state**

In qZSI active state of operation, switch $S_1$, $S_4$, $S_6$ are ON or $S_2$, $S_3$, $S_5$ are ON, when $S_1$, $S_3$, $S_5$ are ON or $S_2$, $S_4$, $S_5$ are ON, the qZSI operates in zero state; when $S_1 - S_6$ are all ON, the qZSI operates in shoot-through

state. The equivalent circuits of the qZSI module during different modes. Where the dc input current is considered at constant. The basic model of quasi impedance source inverter is derived across switching frequency from sub-intervals of three-states.

Hence the active switches are required duty cycle for Turn ON and OFF purpose; at the result lower switching loss and improved system efficiency during operating time. If using the saw tooth carrier method for PWM pulse generation, it does produce more current ripples on inductor side. To avoid this problem the triangular carrier-based method is followed and which has produce small inductor current ripple. The switching frequency 100 KHz is proposed for final design (B. Ge, H. Abu-Rub, *et. al.,* Oct. 2013).

## 3. QUASI-Z-SOURCE CASCADE MULTILEVEL INVERTER

The configuration of MIC based on cascaded qZSI modules fed induction motor is presented in Figure 1. The quasi-Z-source network to the traditional CMI Each qZS-HBI module's operating principle is similar to a standard qZSI, i.e., including shoot-through and nonshoot-through states (J.Anderson,*etal.,*2008). Classical H-bridge inverter operation takes while proposed inverter in non-shoot through states. Whereas quazi impedance source inverter operation takes while shoot through states.

The qZS-CMI owns both the characteristics of qZSI and CMI, that is

$$V_{C1} = \frac{1-D}{1-2D} V_{in} \tag{1}$$

$$V_{C2} = \frac{D}{1-2D_{sh}} V_{in} \tag{2}$$

where, $V_{in}$ is input voltage of one qZS-HBI module; D represents the shoot-through duty ratio per module; $V_{C1}$ and $V_{C2}$ are the average capacitor voltages; $V_{DC}$ is the dc-link voltage of each qZS-HBI and $V_{DC}$ is its peak value; $V_{HX}$ is the qZS-CMI's output voltage per phase; $V_{HXK}$ is the qZS-HBI module's output voltage. The subscript $x \in \{a, b, c\}$ represents the three phases; and $k \in \{1, 2, \text{and } 3\}$ represents the number of cascaded modules per phase in all the following sections.

## 4. MODEL OF INDUCTION MOTOR

The induction motor considered here has a three-phase stator and a squirrel-cage rotor which can be represented by a short-circuited three-phase rotor winding [S.B. Kjær *et. al.,* 2002]. The induction motor state model is expressed by (α, β) coordinates as follows and sectional representation rotor and stator axis diagram is shown in Figure 3.

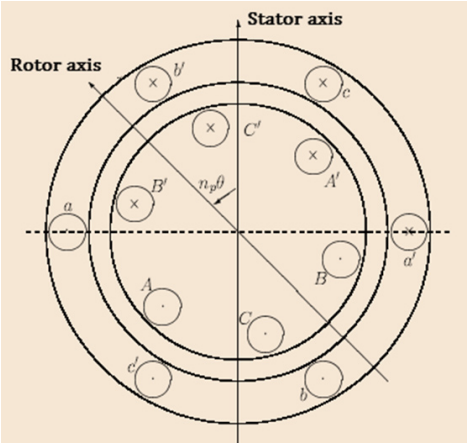


**Figure 3: Axis representation diagram for induction motor**

$$X = A(\omega) \cdot X + B \cdot U \tag{3}$$

$$Y = C \cdot X(4)$$

Where A, B and C are the evolution, the control and the observation matrices respectively.

$$X = [i_{s\alpha} \quad i_{s\beta} \quad \Phi_{r\beta\alpha} \quad \Phi_{r\beta}]^t ; U = \begin{bmatrix} V_{s\alpha} \\ V_{s\beta} \end{bmatrix}; Y = \begin{bmatrix} i_{s\alpha} \\ i_{s\beta} \end{bmatrix}$$

$$A = \begin{bmatrix} -\left(\frac{1}{\sigma T_s} + \frac{1-\sigma}{\sigma T_r}\right) & 0 & \frac{1-\sigma}{\sigma M T_r} & \frac{1-\sigma}{\sigma M}\bar{\omega} \\ 0 & \left(\frac{1}{\sigma T_s} + \frac{1-\sigma}{\sigma T_r}\right) & \frac{1-\sigma}{\sigma M} & \frac{1-\sigma}{\sigma M T_r}\omega \\ \frac{M}{T_r} & 0 & -\frac{1}{T_r} & -\omega \\ 0 & \frac{M}{T_r} & \omega & -\frac{1}{T_r} \end{bmatrix}$$

$$B = \begin{bmatrix} \frac{1}{\sigma L_S} & 0 \\ 0 & \frac{1}{\sigma L_S} \\ 0 & 0 \\ 0 & 0 \end{bmatrix}; C = \begin{bmatrix} 1 & 0 & 0 & 0 \\ 0 & 1 & 0 & 0 \end{bmatrix}$$

With, ω Rotor speed and the machine's parameters are Rs, Rr, M, Ls, Lr and *p*, with:

$$T_r = \frac{L_r}{R_r}, T_s = \frac{L_s}{R_s}, \sigma = 1 - \frac{M^2}{L_s L_r}$$

The mechanical equation is the following:

$$J \cdot \frac{d}{dt}\Omega = C_e - C_r - f \cdot \Omega \tag{5}$$

J is the inertia coefficient, and using the Laplace transform, the equation (5) shows that the relation between the stator flux and the rotor flux represents a low pass with time constant $\sigma T_r$

$$\overline{\Phi_r} = \frac{M}{L_s}\frac{\overline{\Phi_s}}{1 + \sigma T_r s} \tag{6}$$

$$C_e = \frac{3}{2}\frac{p}{2}\left(\Phi_{s\alpha} \cdot i_{s\beta} - \Phi_{s\beta} \cdot i_{s\alpha}\right) \tag{7}$$

The electromagnetic torque can be expressed above.

## 5. DTFC SCHEME FOR INDUCTION MOTOR

The Figure 4 shows the block diagram of the DTFC for induction motor drive with stator resistance estimator. This strategy of control competitive compare to the rotor flux oriented method [S. B. Kjær *et. al.,* 2002].

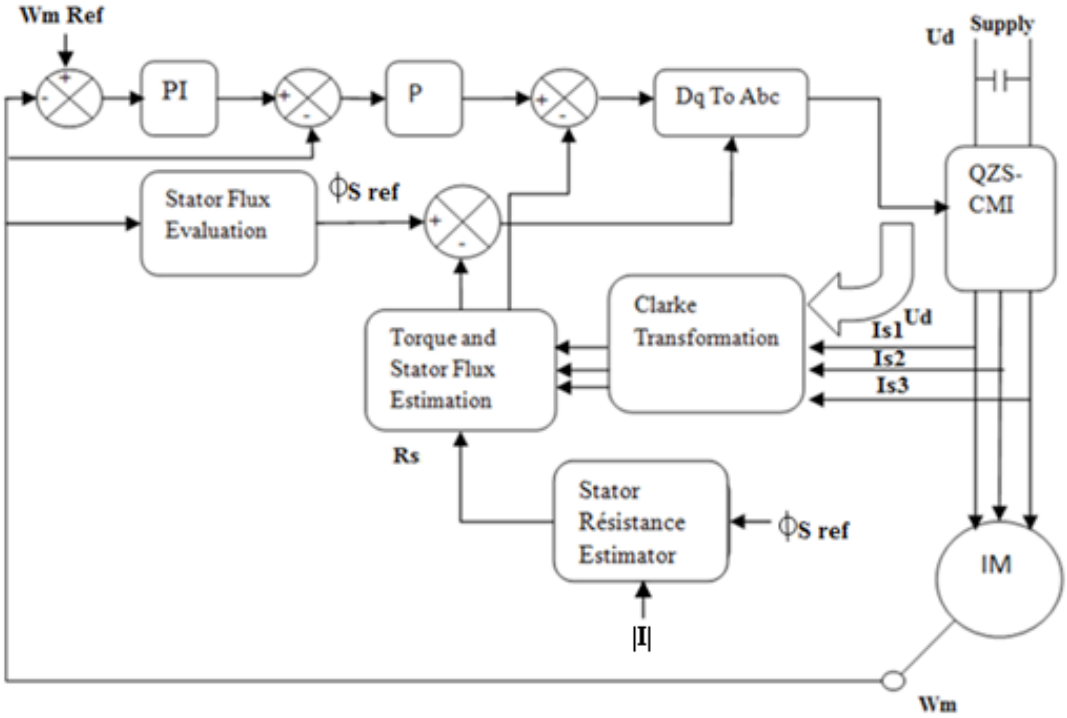


**Figure 4: DTFC block diagram with stator resistance estimator**

The given control a scheme is used to determine the sequence of control on proposed Quasi-z source inverter system. This choice is generally based on the use of hysteresis regulators, whose function is to control the state of the system, and to modify the amplitude of the stator flux and the electromagnetic torque. The stator flux, as given in equation (1), can be approximated as equation (2) over a short time period if the stator resistance is ignored.

$$\bar{\Phi}_s = \bar{\Phi}_{so} + \int_0^t (\bar{V}_s - \bar{R}_s \bar{I}_s)\, dt \tag{8}$$

$$\bar{\Phi}_s \approx \bar{\Phi}_{so} + \int_0^t (\bar{V}_s)\, dt \tag{9}$$

During one period of sampling Te, vector tension applied to the machine remains constant, and thus one can write:

$$\bar{\Phi}_s(\mathrm{K}+1) \approx \bar{\Phi}_s(K) + \int_0^t \bar{V}_s \cdot \mathrm{T}_e \tag{10}$$

Therefore to increase the stator flux, we can apply a vector of tension that is co-linear in its direction and vice-versa. Figure 5 shows the stator flux increment and spatial positions of the voltage vectors keeping the flux inside of the strip hysteresis.

$$\mathrm{Ce} = \frac{3}{2} p \frac{\mathrm{M}}{\sigma \mathrm{L}_s \cdot \mathrm{L}_r} \bar{\Phi}_s \bar{\Phi}_r \sin\gamma \tag{11}$$

If the error of flux is estimate on the direction of stator flux and on a perpendicular direction shown in Figure 6 one puts in evidence the components acting on the torque and on the flux. The component sf$\Delta\Phi$ gives the electromagnetic Torque of the Induction motor while the component sf $\Delta\Phi$ modifies the magnitude of stator flux. The torque is produced by the induction motor can be expressed as equation:

$$Ce = \frac{3}{2} p \frac{M}{\sigma L_s \cdot L_r} \bar{\Phi}_s \bar{\Phi}_r \sin \gamma \tag{12}$$

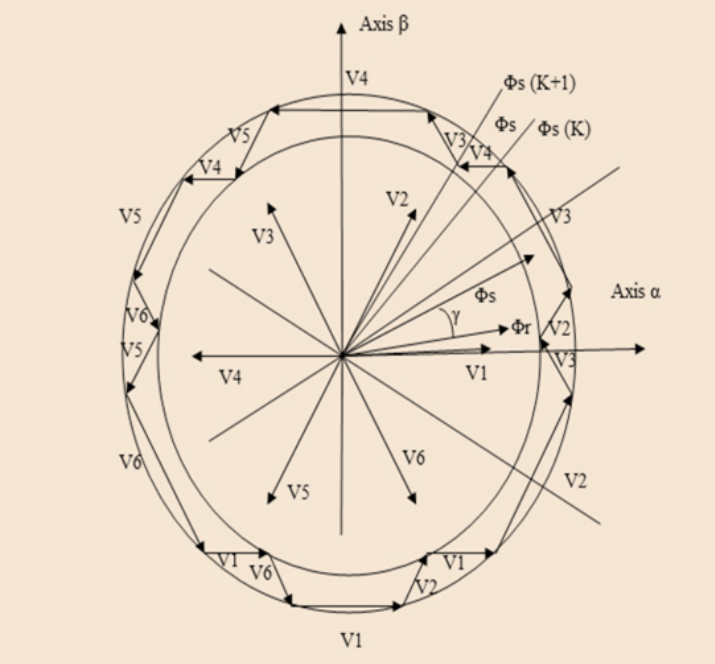


**Figure 5: Stator flux increment and spatial positions of the voltage vectors**

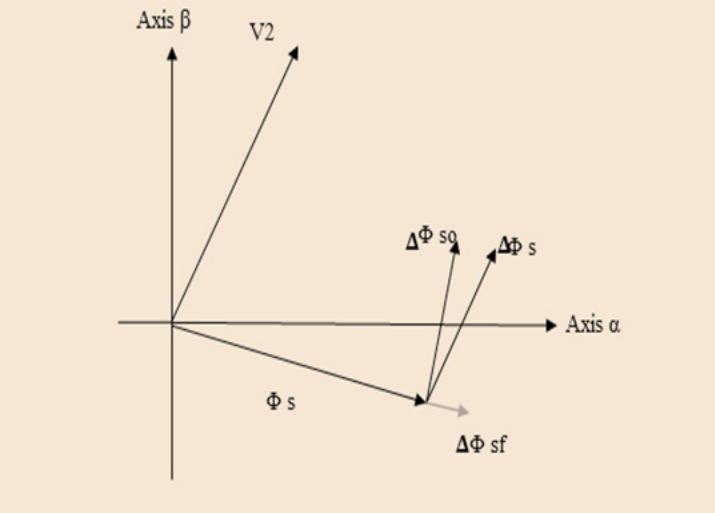


**Figure 6: Components of the error of flux at the time of the application of the vector V2 voltage**

The torque depends upon the amplitude of the two vectors stator flux $\Phi_s$ and rotor flux $\Phi_r$, and their relative position γ. If one succeeds in perfectly controlling the flux $\Phi_s$ (starting with Vs) in module and in position, one can subsequently control the amplitude and the relative position of $\Phi_r$.

## 6. PI RESISTANCE ESTIMATOR FOR DTFC DRIVE

Based on the relationship between change of resistance and change of current, a PI resistance estimator can be constructed in equation (10), as shown in Figure 7.

$$\Delta R_s = \Delta I\left(k_p + \frac{K_i}{s}\right) \tag{13}$$

where, $k_p$ and $k_i$ are the proportional and integral gains of the PI estimator.

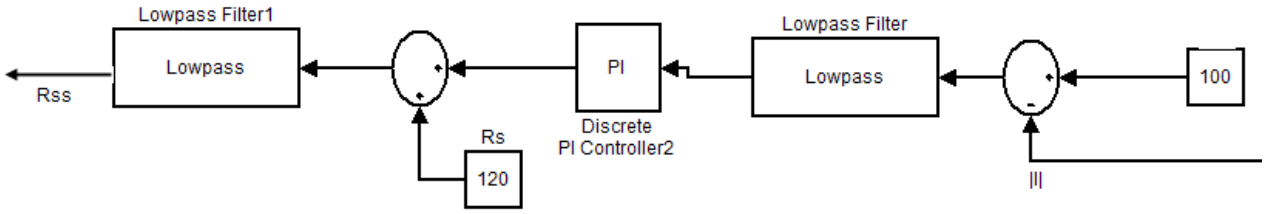


**Figure 7: Block diagram of PI resistance estimator**

When the stator resistance changes, the compensation process can be depicted as, the change of stator resistance will change the amplitude of the current vector. The error of the amplitude of current vector and that of the reference current vector will be used to compensate the change in stator resistance until the error in current becomes zero. Therefore, the steady state error of this resistance estimator is zero. And the reference current vector can be derived from the reference torque and reference flux as

$$I_{ref} = \sqrt{(is_\alpha^*)^2 + (is_\beta^*)^2} \tag{14}$$

$$is_\beta^* = \frac{2}{3}\frac{2}{p}\frac{C_{e\,ref}}{\left|\Phi_{s\,ref}\right|} \tag{15}$$

And $is_\beta^*$ is calculated from the following equation

$$L_s(is_\alpha^*)^2 - \frac{1+\sigma}{\sigma}\left|\Phi_{s\,ref}\right|.is_\alpha^* + L_s(is_\alpha^*)^2 + \frac{\left|\Phi_{s\,ref}\right|^2}{\sigma L_s} = 0 \tag{16}$$

The filter time constant should be small compared to the stator resistance estimator time constant to overcome its effect on the stator resistance adaptation. The final estimated stator resistance $\widehat{R_s}$ is again passed through a low pass filter to have a smooth variation of stator resistance value. This updated stator resistance can be used directly in the controller.

## 7. SIMULATION RESULTS

The simulation model of impedance network fed induction motor is shown in Figure 8. DC voltage interfaced quasi Z-network topology should reduced the stress after Z network the multilevel inverter should reduces the harmonics in three phase line. Furthermore, the qZS multi level inverter choice have been reduced inrush current; since soft starters are offers more economical merits for drive applications but that require speed and torque control only during motor start-up.

Additionally, they are produce the ideal solution for applications where space is a concern, as they usually takes up less space than variable frequency drives. To verify the proposed schemes, three phase MIC seven level cascaded H-Bridge inverter fed induction motor with soft start capability is implemented in Simulink environment and achieves desired soft starting performance. The simulation parameters are given in Table 1. The three phase soft starting current waveform is shown in Figure 9 and Figure 10 show the full load seven-level voltage. Figure 11 and Figure 12 shows the overall performance for induction motor; which has shows phase voltage, stator current, speed and torque. Those are verified in starting time and running condition.

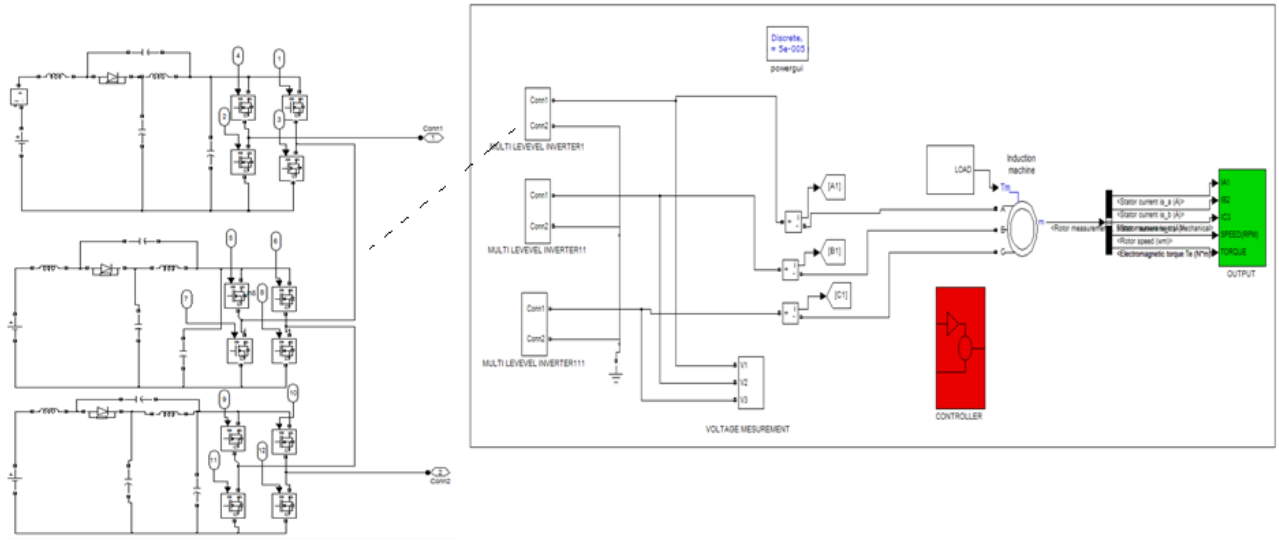


**Figure 8: Simulation Of qZS MLI Fed Induction Motor.**

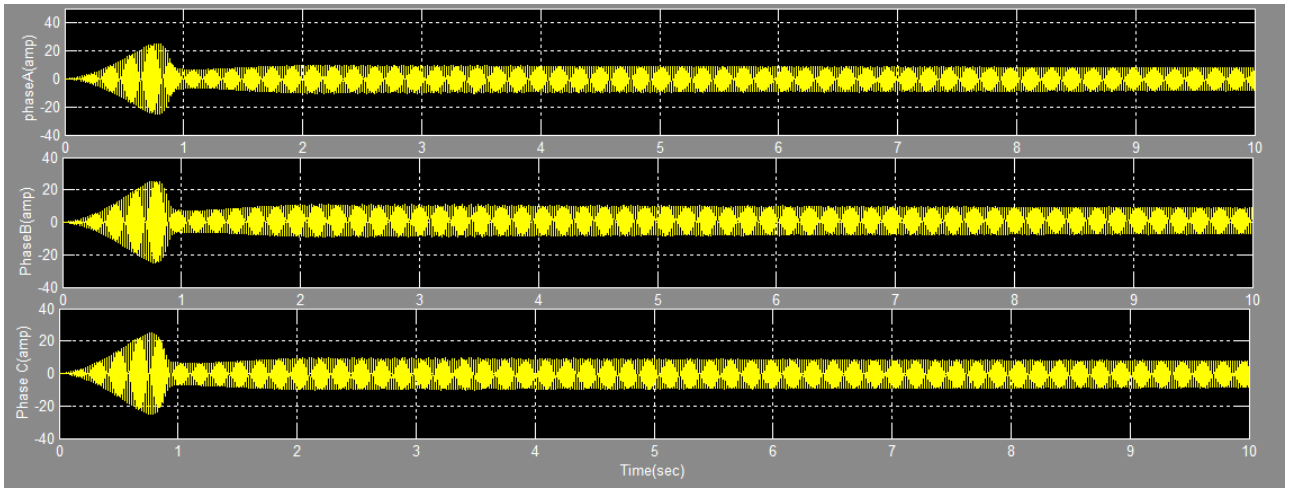


**Figure 9: Waveform for three phase stator current**

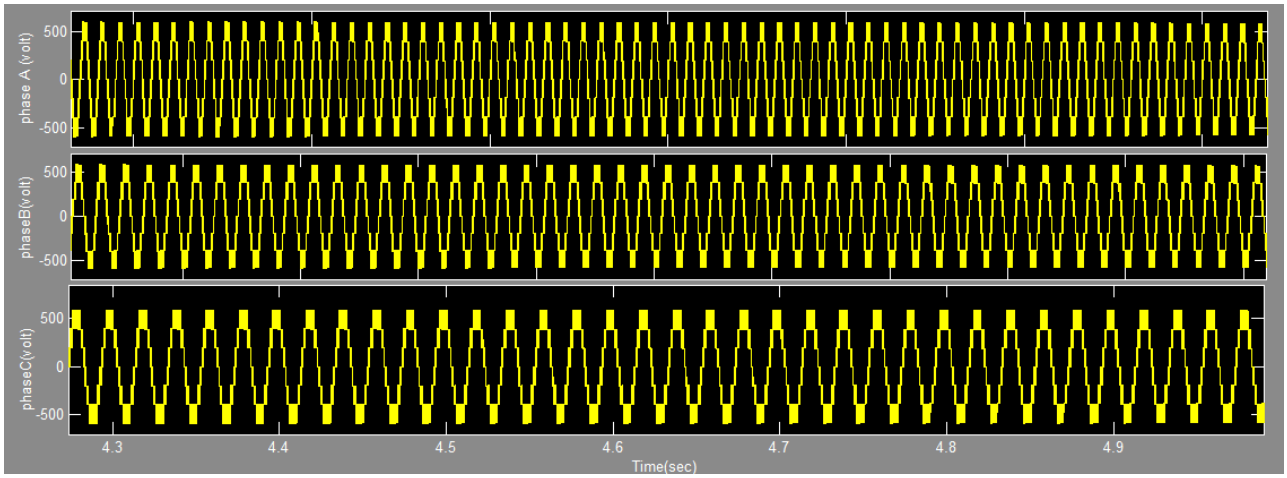


**Figure 10: Three phase multilevel output voltage**

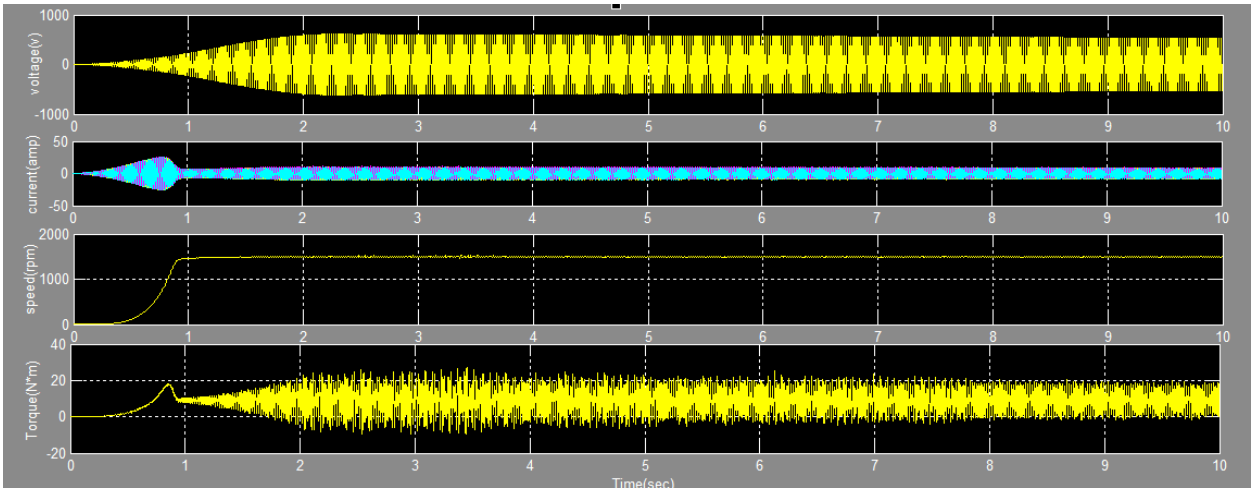


**Figure 11: Overall Motor Performance at Staring Condition**

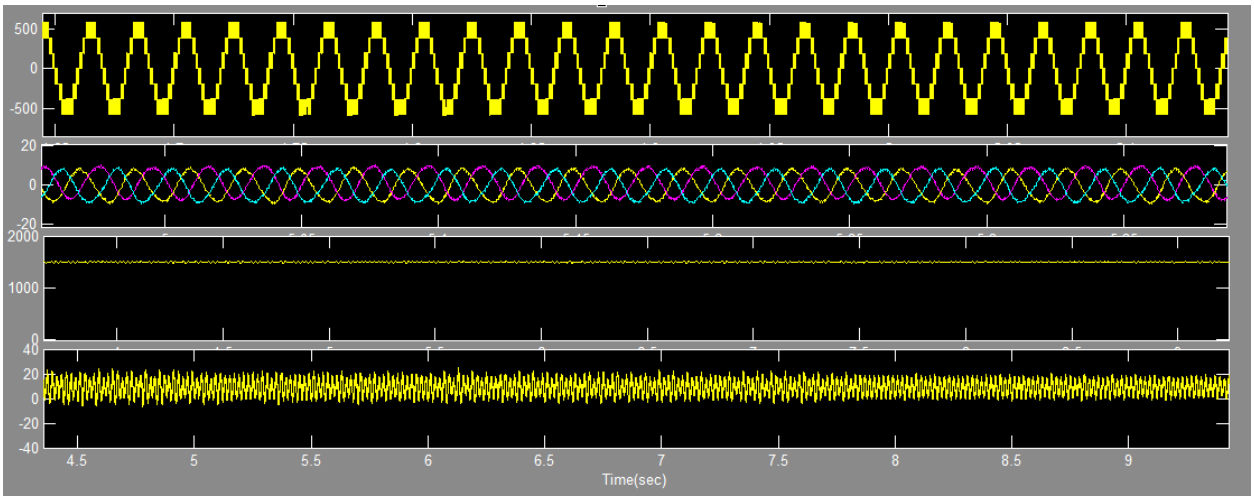


**Figure 12: motor performance at running condition. (Time : 4.5sec to 9.5sec)**

**Table 1**
**Induction Motor Ratings**

| | |
|---|---|
| Power | 2kW |
| Voltage (L – L) | 930 V |
| Current | 8A |
| Frequency | 50Hz |
| Speed | 1440 rpm |
| Torque | 10 N-M |
| Stator resistance ($R_s$) | 1.115Ω |
| Rotor resistance ($R_r$) | 1.083Ω |
| Stator leakage inductance ($Ll_s$) | 0.005974H |
| Rotor leakage inductance ($Ll_s$) | 0.005974H |
| Mutual Inductance between stator and rotor ($L_m$) | 0.2037H |
| Moment of Inertia (J) | 0.02 kg – $m^2$ |
| Viscous Friction (B) | 0.005752N-m/rad.\s |

## 8. CONCLUSION

This paper introduced a *q*ZSI induction motor drive soft starting operation. A qZS-CMI's fed induction motor drive operating under direct torque and flux control (DTFC). The proposed control scheme has achieved soft start capability in induction motor, Quasi Z-source allows continuous input current, improved reliability and achieved desire voltage gain using small shoot-through ratio of the system. Furthermore, the employed cascaded H-bridge inverter is to reduce voltage balancing problem and the seven-level voltages is achieved under full load full condition. Finally, the proposed strategy has been successfully verified and achieved desired simulation results.

## REFERENCE

[1] J. M. Carrasco, L. G. Franquelo, J. T. Bialasiewicz, E. Galvan, R. C.Portillo Guisado, M. A. M. Prats, J. I. Leon, and N. Moreno-Alfonso, Aug. 2006, "power-electronic systems for the grid integration of renewable energy sources: A survey," IEEE Trans. Ind. Electron. , Vol. 53, No. 4, pp.1002–1016.

[2] Singh, G.K. April 1994, "Field-oriented control of induction motors using DSP" IEEE Trans. Ind. Computing & Control Engineering Journal (Volume: 5, Issue: 2).

[3] L.Tang, L.Zhong, M.F. Rahman and Y.Hu, 2002,"A Novel Direct Torque Control Scheme for Interior Permanent Magnet Synchronous Machine Drive system with low ripple in Torque and flux and fixed switching frequency," Conf. Rec. IEEE PESC'02 33rd Power Electronics Specialists' Conference, Cains, Australia, pp.529-534,

[4] I.Takahashi and Y. Ohmori, March/April, 1989,"High Performance Direct Torque Control of an Induction motor,"IEEE Trans Ind. Appl. Vol.IA-25, pp.257-267.

[5] D.Seyoum, F. Rahman and C. Grantham, Jun.2003,"Simplified flux estimation for control application in induction machines, " in Proc. IEEE International Electric Machines and Drives Conference - IEMDC'03,vol. 2, pp. 691-695.

[6] S. B. Kjær, J. K. Pedersen, and F. Blaabjerg, 2002, "Power inverter topologies for photovoltaic modules—A review," in Proc. IEEE IAS, pp.782–788.

[7] Merabet, M. Ouhrouche, and R-T Bui, July. 2006,"Nonlinear Predictive Control with Disturbance Observer for Induction Motor Drive," IEEE International Symposium on Industrial Electronics, Vol. 1, pp. 86 – 91,

[8] G. Zenginobuz, I. Cadirci, M. Ermis, and C. Barlak, June 2004,"Performance Optimization of Induction Motors During Voltage-Controlled Soft Starting", IEEE Transactions on Energy Conversion, Vol. 19, no.2, pp. 278-288.

[9] M. Calais and V. Agelidis, Jul. 1998, "Multilevel converters for single-phase grid connected photovoltaic systems—an overview," in Proc. IEEE Int. Symp. Ind. Electron, pp. 224–229.

[10] M. Shen, A. Joseph, Y. Huang, F. Z. Peng, and Z. Qian, Aug. 14–16, 2006, "Design and development of a 50 kWZ-source inverter for fuel cell vehicles," in Proc.Int. Conf. Power Electron. Motion Control, pp. 1076–1080

[11] L. Liu, H. Li, Y. Zhao, X. He, and Z. J. Shen, Sep. 2011, "1 MHz cascaded Z source inverters for scalable grid-interactive photovoltaic (PV) applications using GaN device," in Proc. IEEE ECCE, pp. 2738–2745.

[12] Y. Liu, B. Ge, H. Abu-Rub, and F. Z. Peng, Feb. 2014,"An effective control method for quasi-Z-source cascade multilevel inverter-based grid-tie single-phase photovoltaic power system," IEEE Trans. Ind. Informat., Vol. 10, No. 1, pp. 399–407.

[13] B. Ge, H. Abu-Rub, F. Peng, Q. Lei, A. de Almeida, F. Ferreira, D. Sun, and Y. Liu, Oct. 2013, "An energy stored quasi-Z-source inverter for application to photovoltaic power system," IEEE Trans. Ind. Electron. , Vol. 60, No. 10, pp. 4468–4481.

[14] Y. Liu, B. Ge, H. Abu-Rub, and F. Z. Peng, Apr. 2014, "Overview of space vector modulations for three-phase Z-source/quasi-Z-source inverters," IEEE Trans. Power Electron., Vol. 29, No. 4, pp. 2098–2108.

[15] J. Anderson and F. Z. Peng, 2008, "Four quasi-Z-source inverters," in Proc.IEEE Power Electron. Spec. Conf. , Jun. 15–19, pp. 2743–2749.